

Renormalization group for Anderson localization on high-dimensional lattices

Boris L. Altshuler^a, Vladimir E. Kravtsov^b, Antonello Scardicchio^{b,c}, Piotr Sierant^d, and Carlo Vanoni^{e,c,1}

This manuscript was compiled on March 5, 2024

We discuss the dependence of the critical properties of the Anderson model on the dimension d in the language of β -function and renormalization group recently introduced in Ref. (1) in the context of Anderson transition on random regular graphs. We show how in the delocalized region, including the transition point, the one-parameter scaling part of the β -function for the fractal dimension D_1 evolves smoothly from its $d = 2$ form, in which $\beta_2 \leq 0$, to its $\beta_\infty \geq 0$ form, which is represented by the random regular graph (RRG) result. We show how the $\epsilon = d - 2$ expansion and the $1/d$ expansion around the RRG result can be reconciled and how the initial part of a renormalization group trajectory governed by the irrelevant exponent y depends on dimensionality. We also show how the irrelevant exponent emerges out of the high-gradient terms of expansion in the nonlinear sigma-model and put forward a conjecture about a lower bound for the fractal dimension. The framework introduced here may serve as a basis for investigations of disordered many-body systems and of more general non-equilibrium quantum systems.

Anderson localization | Renormalization group | Many-body localization

Despite extensive, centuries-long research in the field of statistical mechanics, the mechanisms underlying the process of thermalization are still not fully understood. The analog of the ergodic hypothesis of classical mechanics in quantum mechanical systems, and its validity in presence of quenched disorder, present several counter-intuitive aspects which attracted the interest of the scientific community working on foundations and applications of statistical mechanics. It is known that when the interaction between the particles can be neglected, if the disorder is sufficiently strong, the system undergoes a transition from an ergodic to a localized, Anderson insulator, phase (2–4) which has no counterpart in classical mechanics. The properties of the so-called Anderson transition are qualitatively understood to depend upon the physical dimension of space d and, as the d increases indefinitely, those properties have been a subject of growing interest in the recent past (5–11).

In part, this is due to the interest in the complementary case, in which the elementary excitations of the system *cannot* be thought of as non-interacting particles, and interaction needs to be considered in the analysis. The analog of Anderson localization, in this case, is the subject of Many-Body Localization (MBL) (12–14), where the system develops local integrals of motion (15, 16) and transport is suppressed (17). The connection between MBL and the problem of Anderson localization occurs when thinking of the latter on infinite-dimensional lattices, or expander graphs, such as trees, and regular random graphs (RRG) (18–20). Some of the difficulties in interpreting the numerical data supporting MBL (see for example (21–25)) have very much in common with the difficulties of interpreting the numerical data of the Anderson model on the RRG (where there is no doubt about the existence of the transition (26)).

In part, however, there is another reason for the current interest in the Anderson transition on expander graphs. The absence of an obvious upper critical dimension and the failure of ϵ expansion around $d = 2$ dimensions to fit the numerically found exponents (27) at $\epsilon = 1$ ($d = 3$), despite going to five loops in the sigma model (28), is also puzzling. Such mismatch could be due to a failure of the perturbation theory to converge (29), but it could also be due to something more profound, and reveal a non-trivial behavior of the model in high dimension (30).

In this paper, we build upon the work that some of us did in Ref. (1) and show how a single parameter scaling theory (a modern form of the one presented in Ref. (31)) can explain the numerics on the statistical properties of wave functions and spectrum. We also show, connecting to our work (1) that the irrelevant corrections, in the RG sense, to the one-parameter scaling evolve in the limit of infinite dimensions to give rise to a topologically different RG flow. More specifically, to set the stage,

Significance Statement

Quantum particles can localize when the surrounding environment is sufficiently disordered, a phenomenon named Anderson localization. In this work, we discuss how the properties of the localization transition depend on the dimensionality of real space, showing how to take properly the limit of infinite dimensions. To do so, we use the renormalization group for quantities that are easily accessible numerically via exact diagonalization. The results presented here are the bridge connecting low dimensional systems, amenable to controllable analytical treatment, and infinite dimensional systems, relevant for interacting disordered systems. Moreover, the method developed in this work allows for a quantitative analysis of numerical data for the Many-Body Localization problem and can help resolve discrepancies still existing in this problem.

Author affiliations: ^aPhysics Department, Columbia University, 538 West 120th Street, New York, New York 10027, USA; ^bICTP, Strada Costiera 11, 34151, Trieste, Italy; ^cINFN Sezione di Trieste, Via Valerio 2, 34127 Trieste, Italy; ^dICFO-Institut de Ciències Fotòniques, The Barcelona Institute of Science and Technology, Av. Carl Friedrich Gauss 3, 08860 Castelldefels (Barcelona), Spain; ^eSISSA – International School for Advanced Studies, via Bonomea 265, 34136, Trieste, Italy

¹To whom correspondence should be addressed. E-mail: cvanoni@sissa.it

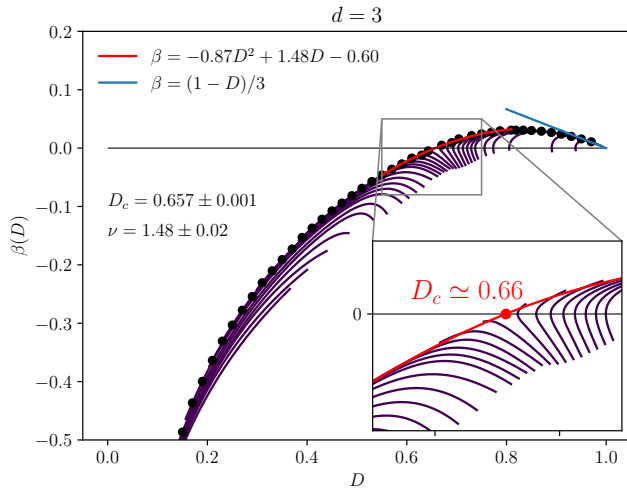


Fig. 1. Renormalization group (RG) trajectories (solid lines) for 3d Anderson model obtained from the numerical calculation of the eigenfunction Shannon entropy $S(L)$ and the corresponding finite-size fractal dimension $D(L) = dS(L)/d \ln N$. The envelope of RG trajectories (black dots) is the single-parameter β -function $\beta(D)$. Its root D_c gives the fractal dimension of the critical wave functions and the slope of the red solid curve at $D = D_c$ determines the relevant critical exponent ν . The slope of $\beta(D)$ at the ergodic fixed point $D = 1$ (blue solid line) is $(d - 2)/d = 1/3$. The accuracy of one-parameter scaling can be inferred from the length of the initial parts of the trajectories, ‘the hairs’, before merging with the single-parameter curve.

we first recall the scaling theory of Abrahams, Anderson, Licciardello, and Ramakrishnan (31), where the RG flow for the dimensionless conductance has been discussed for the first time. We then present how to extend the theory to spectral observables, that are more easily accessible numerically and that are equivalent to the dimensionless conductance, under the one-parameter scaling hypothesis. We argue that the fractal dimension of the eigenstates is a good observable for our purposes and we describe some general properties of its flow under the renormalization group. While its behavior can be predicted analytically in some regimes (as in the deep ergodic and localized regimes), we have to rely on numerical results for the properties near the critical point. We show that our framework is compatible with the existing numerical observations and gives a clear picture of the behavior of the model as the number of spatial dimensions is increased. This is achieved by matching the known exact results in $2d$ – and perturbations away from it in the ϵ -expansion framework – to the results on random regular graphs, that we argue to be the correct limit $d \rightarrow \infty$.

Main results

The main result of the paper is the numerical calculation for three and the higher dimensions $d = 4, 5, 6$ of the β -function, defined as

$$\beta(D) = \frac{d \ln D}{d \ln N}, \quad [1]$$

where $D = D_1(L)$ is the finite-size fractal dimension defined as the derivative $D_1(L) = dS(L)/d \ln N$ of the eigenfunction Shannon entropy $S(L)$ with respect to the logarithm of the system volume $N = L^d$. An example for $d = 3$ is presented in Fig. 1.

The β -function that corresponds to a single-parameter scaling is an *envelope* of RG trajectories parametrized by

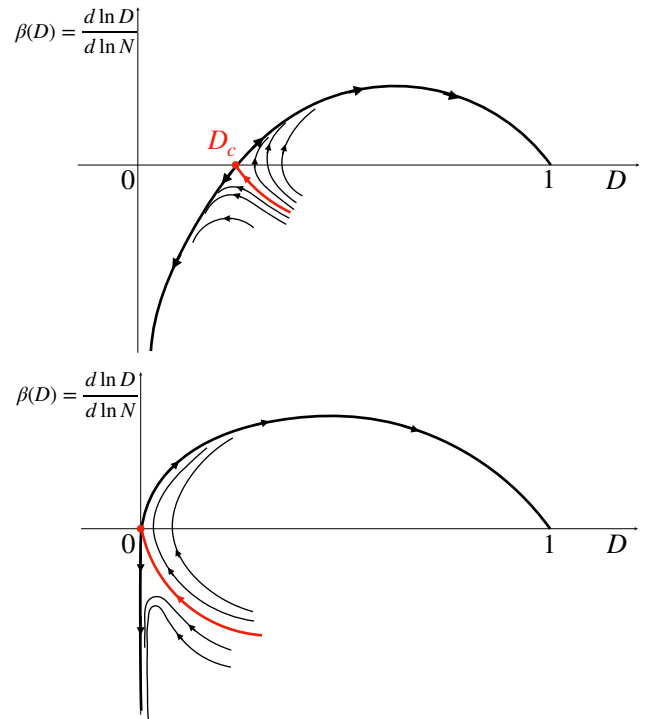


Fig. 2. A sketch of the full β -function. (Upper panel) Behavior at finite dimension, where $0 < D_c < 1$ and the irrelevant direction at finite size becomes increasingly important as d grows. (Lower panel) Behavior on expander graphs (as the RRG), where, near the critical value of W , the irrelevant direction becomes the only one accessible at the available system sizes. The critical fractal dimension $D_c \sim 1/d$ for finite d and vanishes in the $d \rightarrow \infty$ limit, as in expander graphs. Also, the contribution of the irrelevant exponents becomes larger when d grows, ultimately becoming marginal when $d \rightarrow \infty$. This is reflected by the length of the critical trajectory, depicted in red.

the size of the system. The initial part of each trajectory corresponds to small system sizes and is governed by the set of irrelevant exponents y_n . We identify the irrelevant exponents as originating from the high-gradient terms that emerge in the derivation of the effective field theory of localization (32, 33) but are omitted in the non-linear sigma-model. The length of the initial part of trajectories increases when the irrelevant exponent decreases in the absolute value. We show that the principal irrelevant exponent $y = -2 + 2\epsilon + O(\epsilon^2)$ increases (decreases in the absolute value) as the dimensionality $d = 2 + \epsilon$ increases and finally it becomes marginal in the RG sense for the case of random regular graph (1), which corresponds to the limit $d \rightarrow \infty$ (see Fig. 2).

We also conjecture that the critical fractal dimension D_c (see Fig. 1) has the lower bound $D_c \geq 1/d$ and that the slope α_c of $\beta(D)$ at $D = D_c$ is finite $\alpha_c \rightarrow 2$ in the limit $d \rightarrow \infty$. If correct, the existence of such lower bound leads to the scenario I in Ref. (1) and to the existence of two critical lengths for localization transition on RRG.

Anderson Model and scaling theory for conductance

In this work, we consider the Anderson model as originally introduced in Ref. (2). It describes a single quantum particle (whose statistics is thus not important) hopping on a given lattice Λ in the presence of onsite random fields. In the case of a d -dimensional cubic lattice, that we study in this work,

the volume of the system (i.e. the number of sites) is $N = L^d$. The Hamiltonian operator defining the model is

$$H = -J \sum_{\langle i,j \rangle \in \Lambda} |i\rangle\langle j| + \text{h.c.} + \sum_{i \in \Lambda} \epsilon_i |i\rangle\langle i|. \quad [2]$$

In the above expression, $\langle \cdot \rangle$ represent nearest neighbor sites on the lattice Λ and the on-site energies ϵ_i are distributed uniformly according to the box distribution $g(\epsilon) = \theta(|\epsilon| - W/2)/W$. We choose the hopping rate as the unit of energy, $J = 1$. The eigenstates ψ_n have energy $H|\psi_n\rangle = E_n|\psi_n\rangle$.

It is known that the model can have a transition from diffusive/ergodic to localized/non-ergodic phase as the variance – or strength – of disorder W increases. The location of such transition (i.e. the critical value of $W = W_c$) strongly depends on the structure of the lattice Λ , while the critical exponents at the transition are universal and depend only on the lattice dimensionality. In the seminal work (31) (often called the ‘‘Gang of Four’’ paper) the dependence of dimensionless conductance on the system size and the strength of disorder has been investigated for different spatial dimensions d . The main result of the paper which determined the development of the field for decades, was a formulation of the single-parameter scaling. It stated that the ‘speed’ of the evolution of conductance with the system size depends only on the conductance itself and not on the system size and the disorder strength separately. This allowed to uncover the crucial role of lattice dimensionality d and predict the absence of delocalized states in the thermodynamic limit for $d = 1$ and $d = 2$, as well as the existence of the localization/delocalization transition for $d > 2$.

In Ref. (31) the main observable is the dimensionless conductance $g(L)$, where L is the linear size of the system. $g(L)$ is defined as the ratio:

$$g(L) = \frac{E_{Th}}{\delta} = \frac{2\hbar}{e^2} \sigma L^{d-2}$$

where \hbar/E_{Th} is the time it takes for a wave packet to reach the sample boundary, δ is the mean level spacing and σ is the conductivity. The mathematical formulation of the single parameter scaling is then given by the equation:

$$\frac{d \ln g(L)}{d \ln L} = \beta(g(L)), \quad [3]$$

where $\beta(g)$ is the parameter-free β -function.

Already from the definition of $g(L)$, it is easy to see that in the developed metallic regime (where σ is L -independent), the β -function is a positive constant $\beta(g) = (d - 2)$. In the deep insulator regime $\sigma \sim \exp(-L/\xi)$, the β -function is $(-L/\xi) = \ln(g)$ is negative. A continuous interpolation between these two regimes for $d > 2$ inevitably leads to the unstable fixed point g_c such that $\beta(g_c) = 0$ which corresponds to the localization/delocalization transition. If for small system sizes the initial value is $g_0 > g_c$, the conductance $g(L)$ increases with L driving the system to the metallic regime, while at $g_0 < g_c$ the conductance decreases with L and, eventually, the system reaches the deep insulating regime. In contrast to this scenario, if $d < 2$ (e.g. $d = 1$) the β -function is everywhere negative and the metallic behavior is not possible. The case of the two-dimensional lattice is special, as at $g \rightarrow \infty$ we have $\beta(g) \rightarrow 0$ (e.g. $d = 2$ is a critical dimensionality). A more careful perturbative study

in $1/g$ shows that for disordered potentials without spin-orbit interaction this limit is reached from below, so that the simplest assumption of a monotonic β -function leads to the conclusion that $\beta(g) < 0$ everywhere, e.g. on the absence of delocalized states for $d = 2$. Expanding the β -function around $g = g_c$ it is possible to determine some critical properties, such as the exponent $\nu = 1/s$, where s is the logarithmic slope of the β -function at the critical point $\beta(g) = s \ln(g/g_c)$. For more details, we refer to (31).

β -function for ‘modern’ observables

Numerically accessible scaling variables. The Anderson localization transition affects most observable properties of the system. The onset of the localized phase can be spotted not only from the absence of transport (as in the original work by Anderson (2)), but also through properties of the spectrum and statistics of eigenfunction. The conductance has a transparent physical meaning but it is not easy to compute numerically. It can be found using the Kubo formula in terms of numerically obtained eigenstates or, alternatively, using Green functions, as proposed by Lee and Fisher (34).

Modern libraries for high-performance computing make spectral statistics and eigenfunctions statistics more readily accessible and therefore preferable. Trusting the *one parameter scaling hypothesis*, these properties are on the same footing as the conductance in describing the RG flow of the properties of the system.

A natural observable for eigenfunctions properties is the Shannon entropy:

$$S_n^{(1)} \equiv S_n = - \sum_i \psi_n^2(i) \ln(\psi_n^2(i)), \quad [4]$$

(where $\psi_n(i) = \langle i|\psi_n\rangle$) or eigenfunction Renyi entropy:

$$S_n^{(q)} = \frac{1}{1-q} \ln \sum_i |\psi_n(i)|^{2q}, \quad [5]$$

and their derivatives with respect to the logarithm of volume $N = L^d$.

The derivative $D(L)$ with respect to $\ln N$ of the average value S of the eigenfunction Shannon entropy is a fundamental quantity. In the limit $N \rightarrow \infty$ it gives the fractal dimension of the eigenfunction support set, which is equal to:

$$D_1 \equiv \lim_{N \rightarrow \infty} \frac{dS^{(1)}}{d \ln N} = \begin{cases} 1, & \text{ergodic states} \\ < 1, & \text{(multi)fractal states} \\ 0, & \text{localized states} \end{cases} \quad [6]$$

The corresponding derivative of the average eigenfunction Renyi entropy is the eigenfunction fractal dimension D_q which gives important details of the multifractal eigenfunction distribution.

The special role of D_1 is seen from its connection with the spectral property of level compressibility defined as $\chi = \langle \delta n^2 \rangle / \langle n \rangle$, where n is the number of energy levels in a given energy window and the average is over different positions of the energy window and over disorder realizations. It was shown (35) that for weak multifractality near the ergodic phase, the level compressibility is related to the fractal dimensions as $\chi \approx (1 - D_2)/2$. However, in this regime, it is degenerate with respect to q , namely $(1 - D_2)/2 = (1 - D_q)/q$. Later on, it has been shown analytically in Refs. (36, 37) that

for some random matrix models where both χ and D_q are known, only D_1 satisfies the relation with χ , even for strong multifractality. Therefore we are led to suppose that D_1 has a spectral implication, in contrast to D_q with $q \neq 1$.

In view of a fundamental role of D_1 we choose, instead of $g(L)$, the scaling variable $D(L)$ defined as an analogue of D_1 :

$$D(L) = \frac{dS(L)}{d \ln N}, \quad [7]$$

where $S(L)$ is the average eigenfunction Shannon entropy at size L .

From the above discussion, it is clear that $D(L)$ is intimately related to spectral statistics. Among other spectral statistics the most popular recently was the r -parameter introduced in Ref. (38) and defined starting from the spectrum E_n and the gaps $\Delta E_n = E_{n+1} - E_n$,

$$r = \frac{1}{N-2} \sum_{n=1}^{N-2} \frac{\min(\Delta E_n, \Delta E_{n+1})}{\max(\Delta E_n, \Delta E_{n+1})}. \quad [8]$$

When E_n 's are eigenvalues of a real Hamiltonian, the average of r takes values between $r_{\text{GOE}} \simeq 0.5307$ and $r_{\text{P}} = 2 \ln 2 - 1 \simeq 0.386$. When $r = r_{\text{GOE}}$ the spectrum behaves according to the predictions of random matrix theory (Gaussian orthogonal ensemble) and we expect the system dynamics to be ergodic. If instead $r = r_{\text{P}}$, the energy levels are distributed independently (absence of level repulsion) and ergodicity is broken. Across the Anderson transition, the value of r goes from r_{GOE} at small W to r_{P} at large W .

We would like to mention here an important difference between the r parameter statistics and the spectral compressibility that is related to $D(L)$. The point is that the former is defined at a small energy scale of the order of the mean level spacing δ , while the latter (and presumably also $D(L)$) knows about level correlations at a scale much larger than δ . This is important for sensing the multifractal-to-ergodic transition which in some cases does not show up in the r -statistics, as it happens, e.g. in the Rosenzweig-Porter random matrix model (39).

For this reason, we choose in this paper the variable $D(L)$ as the scaling parameter that stands for the dimensionless conductance in the RG equation:

$$\frac{d \ln D(L)}{d \ln N} = \beta(D(L), L). \quad [9]$$

Our goal is to compute numerically the l.h.s. of Eq. (9), without any *a priori* assumption about the single-parameter scaling. The single-parameter scaling implies that the β -function depends only on $D(L)$ and thus the solution $L(D)$ of this equation is a single-valued function. The inverse function $D(L)$ may be few-valued, but in any case it should be represented by a single parametric curve. On the contrary, if there are other (hidden, or irrelevant in the RG language) parameters, there will be a family of curves satisfying Eq. (9), each curve corresponding to a certain initial condition. Thus numerical evaluation of the l.h.s. of Eq. (9) provides a framework for answering the question about the nature of the transition, allowing to discern single- from multiple-parameter scaling.

Before we come to numerics, we would like to review the general properties of the β -function if the single-parameter scaling is given for granted.

General properties of $\beta(D)$. In the localized phase, when $D \ll D_c$, and in particular when $D \rightarrow 0$, the eigenfunctions decay exponentially with the distance from the localization center $\psi(r) = A r^{-\alpha} \exp[-r/\xi]$. Moreover, in finite spatial dimension d , the number of sites at a given distance r grows as $n(r) \sim r^d$. Therefore, the participation entropy becomes

$$\begin{aligned} S &\equiv - \left\langle \sum_x \psi^2(x) \ln \psi^2(x) \right\rangle \\ &\simeq - \sum_{r=0}^L n(r) A r^{-\alpha} e^{-r/\xi} \ln(A r^{-\alpha} e^{-r/\xi}) \\ &= - \ln A + \sum_{r=0}^L n(r) A r^{-\alpha} \left(-\alpha \ln r - \frac{r}{\xi} \right) e^{-r/\xi}, \quad [10] \end{aligned}$$

with $\sum_{r=0}^L n(r) A r^{-\alpha} e^{-r/\xi} = 1$ from the wavefunction normalization. From the definition of $D(L)$, Eq. (7), and neglecting the logarithm in Eq. (10), being subleading, we get

$$D \simeq \frac{L^{2-\alpha} n(L)}{\xi^d} A e^{-L/\xi} \simeq \left(\frac{L}{\xi} \right)^{d+2-\alpha} e^{-L/\xi}, \quad [11]$$

and using this result, the β -function turns out to be

$$\beta(D) = \frac{1}{d} \ln D - \frac{d-\alpha+2}{d} \ln |\ln D| + O(1), \quad D_c \gg D \gtrsim 0. \quad [12]$$

At not very large $d \sim 1$ and $\alpha \sim 1$ the first term makes the leading contribution to $\beta(D)$ in the insulator. At large d and close to criticality the exponent $\alpha = d - d_1$, as the structure of the wave function inside localization radius is close to that of a critical one and thus upon averaging over the volume $r^d < \xi^d$ it acquires a power-law prefactor $r^{d_1}/r^d = r^{-(d-d_1)}$. According to our conjecture $1 < d_1 < 2$ formulated later on in this paper, we have $1 < d - \alpha < 2$ and it is finite in the limit $d \rightarrow \infty$. Thus the first term in Eq. (12) remains the leading one also for large d . It is important to note that the region of applicability of Eq. (12) shrinks to zero in the limit $d \rightarrow \infty$. This is a clear indication of the failure of single-parameter scaling to describe this limit properly.

In the other limiting case $D \rightarrow 1$ we have $\beta(D) \simeq \alpha_1(1 - D)$. The slope α_1 is fixed by the results of the ‘‘Gang of Four’’ (31). Close to the metallic limit in the orthogonal ensemble, the corrections to D must be proportional to the inverse of the dimensionless conductance:

$$D \approx 1 - c/g \simeq 1 - c'/L^{d-2}. \quad [13]$$

This means that

$$\beta_d(D) = \frac{d-2}{d} \frac{1-D}{D}, \quad D \lesssim 1, \quad [14]$$

which gives

$$\alpha_1 = \frac{d-2}{d} \quad [15]$$

near $D = 1$. In the limit $d \rightarrow \infty$ one obtains $\alpha_1 = 1$, the same scaling we find in RMT and for expander graphs (1, 10). At $d = 2$ we obtain $\alpha_1 = 0$; we investigate more in detail the consequences of this observation later. Notice also that the above result obtained using a scaling argument can also be found performing the ϵ -expansion around $d = 2$, as shown

later.

At the Anderson localization transition (and in general close to an unstable fixed point of the RG equations) we must have

$$\beta(D) = \alpha_c(D - D_c), \quad [16]$$

where we are assuming that $\beta(D)$ vanishes with a finite derivative; such assumption is valid in any finite dimension but is not necessarily true in the $d \rightarrow \infty$ limit (1). Later on we argue that, for short-range models like the Anderson model on a d -dimensional lattice, α_c remains finite in this limit.

The slope α_c determines the finite-size scaling exponent ν . Indeed, plugging Eq. (16) into Eq. (9) and setting $D \approx D_c$ one finds the solution:

$$\ln|D - D_c| - \ln|D_0 - D_c| = \alpha_c D_c d \ln L, \quad [17]$$

where D_0 is the value of $D(L)$ at the smallest $L \sim 1$. Then one readily obtains:

$$D = D_c \pm (L/\xi)^{1/\nu}, \quad \xi \sim |D_0 - D_c|^{-\nu} \sim |W_0 - W_c|^{-\nu}. \quad [18]$$

where ν is the finite-size scaling exponent:

$$\nu = 1/(\alpha_c d D_c). \quad [19]$$

The values of α_c and D_c depend on d and must be found from the numerics.

β -function in two dimensions

After having presented some general properties of the β -function in the previous section, we conduct here a more detailed analysis of its behavior at the lower critical dimension $d = 2$.

The β -function in $d = 2$ is always negative and it has a shallow fixed point at $D = 1$ (see Eq. 12 and Eq. 15)

$$\beta_2(D) = \begin{cases} \frac{1}{2} \ln D + O(1), & \text{if } D \ll 1 \\ -a(1 - D)^2, & \text{if } D \simeq 1. \end{cases} \quad [20]$$

From the numerics, we find $a \simeq 1$ (see Fig. 5), which we will assume now to be the case, in agreement with sigma-model calculations, in particular Eq. (32).

Let us consider the behavior at small W (i.e. near $D = 1$). Inserting $-(1 - D)^2$ into r.h.s. of the RG Eq. (9) we find:

$$d \left(\ln L^2 + \frac{1}{1 - D} \right) = 0. \quad [21]$$

This means that

$$\begin{aligned} \xi &= L \exp \left(\frac{1}{2(1 - D(W, L))} \right) \\ &= \ell \exp \left(\frac{1}{2(1 - D(W, \ell))} \right), \end{aligned} \quad [22]$$

is constant along the RG trajectory which is fixed by initial conditions, *i.e.* by the value of r.h.s. of Eq. (22) at the smallest length $L = \ell$ where the single-parameter scaling is still valid (an ultraviolet cutoff). This is the localization length. To see its W dependence at small W we assume that:

$$D(W, \ell) = 1 - (W/W_0)^2 + O(W^3), \quad [23]$$

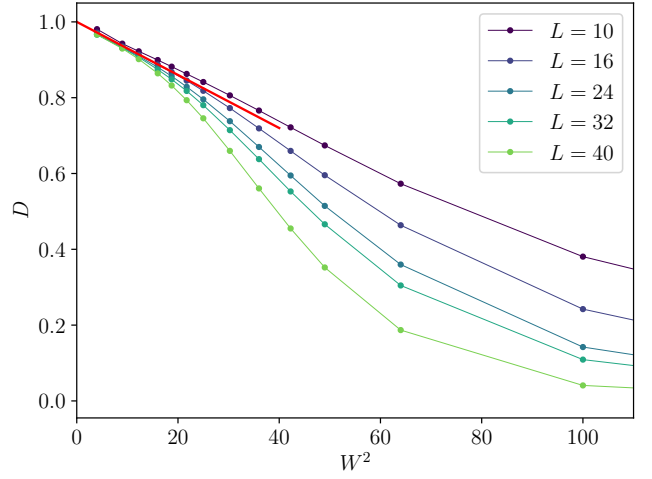


Fig. 3. Fractal dimension extracted from the participation entropy according to Eq. 7. It is clearly visible that near $D \simeq 1$ the dependence is of the form $D = 1 - aW^2$, as indicated by the red line.

as one can see in Fig. 3 (the constant W_0 depends on the cutoff ℓ).

This could have been inferred from the fact that, at finite L , when $W \rightarrow 0$ all the observables are analytic in the variance and therefore must depend on W^2 analytically. This implies that, at small W , one obtains:

$$\xi = \ell \exp \left(\frac{W_0^2}{2W^2} \right). \quad [24]$$

This is in agreement with the well-known weak-localization result that in two dimensions $\ln(\xi/\ell)$ is proportional to the Drude conductivity and thus to the mean free path (MFP). Indeed, from a simple calculation of the decay rate of a wave packet with definite momentum (in the middle of the band), we have $\ell_{\text{MFP}} = v t_{\text{MFP}}$

$$\frac{\hbar}{t_{\text{MFP}}} = N \int d^2 k' \delta(E_k - E_{k'}) |\langle k | \hat{V} | k' \rangle|^2 \propto W^2, \quad [25]$$

where \hat{V} is the on-site potential and $|k\rangle$ is the plane wave of momentum k . This gives $\ell_{\text{MFP}} \sim 1/W^2$ and therefore $\ln(\xi) \sim 1/W^2$, as seen for example in (41).

We now consider the behavior at large W . In this regime we have according to Eq. (12):

$$\beta(D) \simeq \frac{1}{2} \ln D, \quad [26]$$

which is compatible with a solution of the form $D \sim (1/W)^L = \exp[-L/\xi]$, where

$$\xi \simeq \frac{1}{\ln W}. \quad [27]$$

The complete dependence of ξ on W , therefore, has to interpolate between $\xi \sim \exp(c/W^2)$, which is the *weak localization regime* and $\xi \sim 1/\ln W$, which is the *strong localization regime*. Therefore, the complete functional dependence should pass through a region of deceleration. We believe this has led to some claims in the literature that the

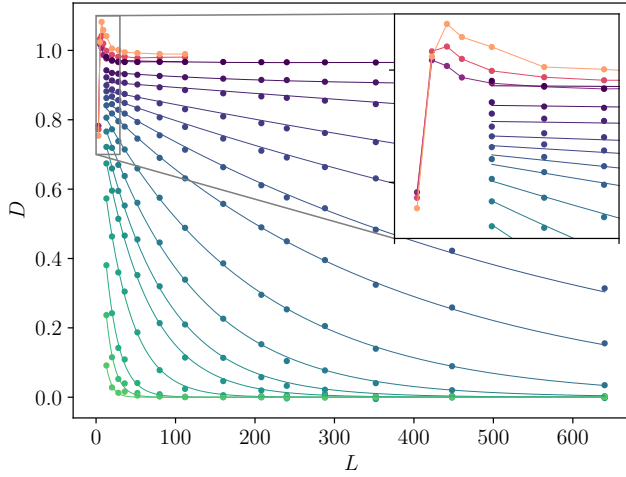


Fig. 4. System size dependence of $D(L)$ in $d = 2$, for different values of W . The solid lines in shades of green are interpolations of the data, used to produce the β -function in Fig. 5. For small sizes and small W , $D(L)$ may exceed $D = 1$ even if the system is localized in the thermodynamic limit, as shown in the inset by the red-shaded curves. This behavior can be obtained analytically if the eigenfunction inside the localization radius is weakly multifractal. It happens because of the ‘basin’ regions where the eigenfunction amplitude $\psi^2 \sim N^{-1-\eta}$ decreases with the volume faster than N^{-1} . Such regions should have a large enough probability to overcome the dominance of the ergodic regions with $\psi^2 \sim N^{-1}$ in the normalization sum $\sum_r \psi(r)^2 = 1$. The job to suppress the probability of ergodic regions is done by the regions with ‘elevated’ $\psi^2 \sim N^{-1+\eta}$ which are always present in a weakly multifractal state together with the ‘basin’ areas. A similar behavior of $D(L)$ is present in the Rosenzweig-Porter random matrix ensemble (39, 40).

scaling $\ln \xi \sim 1/W^\mu$ with μ close or even equal to 1 (42).

Finally, we present the numerical results on the L -dependence of $D(L)$ and obtain the β -function for a two-dimensional system. The set of data on the L -dependence of $D(L)$ for different W obtained from Eq. (7) is presented in Fig. 4, where the eigenfunction Shannon entropy is computed from Eq. (4) using the eigenfunctions from the exact diagonalization of the Anderson model and averaging over disorder and eigenfunctions. From this set of data we obtain the plot $\beta(D)$ vs D which is presented in Fig. 5. Remarkably, all the RG trajectories lie almost exactly on a single curve, just corroborating the single-parameter scaling as a very precise approximation in $d = 2$.

β -function for higher dimensions

Numerical β -function for $d = 3, 4, 5, 6$. The same procedure of numerical computing of β -function can be applied to higher dimensions, albeit with an accuracy that decreases as d increases. The results are presented in Fig. 6 and Fig. 7 as well as in Fig. 1 presented earlier in this paper.

Analyzing the results, we were able to extract the parameters D_c , α_c and ν of a single-parameter curve and compare them with the available numerical results for ν in Table 1. Surprisingly, the value of ν for $d = 3, 4, 5, 6$ extracted from the best fit of a single-parameter curve $\beta(D)$ close to critical point $D = D_c$ is very close to that described by the ‘semiclassical self-consistent theory’ $\nu = 1/2 + 1/(d-2)$, albeit the theory itself is seriously flawed.

Another important result of our numerics is that the effect of the irrelevant exponent (encoded in the length of the RG

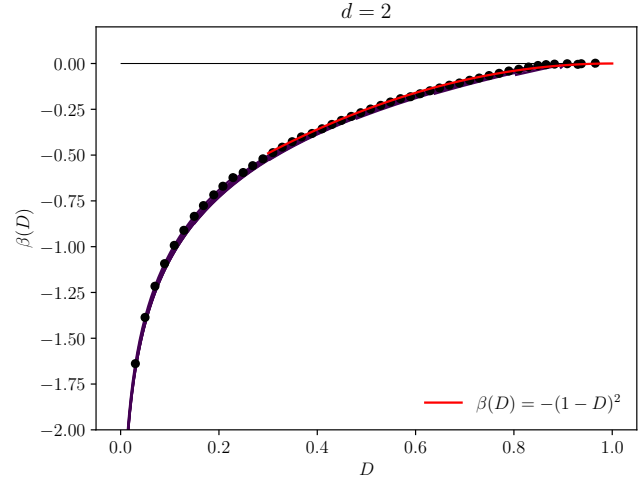


Fig. 5. Plot of the $\beta(D)$ for the Anderson localization model on a two-dimensional lattice. The dark lines are the numerical results, that are obtained from the participation entropy according to the definition, and the black dots are the envelope of the data, identifying the one-parameter scaling part of the β -function. In particular, the fractal dimension is computed by applying the discrete derivative to S , and the resulting points are interpolated using a Padé fit for $W < W_c$ and an exponential fit for $W > W_c$ (see Fig. 6 for more details on the interpolations). The red curve is $\beta(D) = -(1 - D)^2$, which perfectly fits the data and coincides with the correction given by the sigma model, according to Eq. (32)

trajectory at $W = W_c$ before it hits the fixed point) increases as d increases (see also Fig. 9).

$\beta(D)$ in the ϵ -expansion and self-consistent theories

In this Section, we discuss the relationship between our analysis and previous analytical results obtained within the sigma-model formalism. The discussion is necessarily technical and relies on results presented in the literature. The large- d limit and the relation with expander graphs will be investigated in the next Section.

ϵ -expansion within non-linear sigma-model. Let us now move perturbatively away from $d = 2$. Here we employ the results of Refs.(43, 44) in $d = 2 + \epsilon$ dimensions which are based on the nonlinear sigma model formalism. In the orthogonal symmetry class, they read:

$$-\frac{d \ln t}{d \ln L^d} = \frac{\epsilon}{d} - \frac{2}{d} t - \frac{12\zeta(3)}{d} t^4 + O(t^5), \quad [28]$$

$$1 - D_q^{(c)} = \frac{q\epsilon}{d} + \frac{\zeta(3)}{4d} q(q^2 - q + 1)\epsilon^4 + O(\epsilon^5), \quad [29]$$

where $t(L)$ is the inverse dimensionless conductance, using the same notation as in the literature, and $D_q^{(c)}$ is the q -th fractal dimension at $W = W_c$.

Now we introduce the scale-dependent fractal dimension $D_q(L)$ away from the criticality and find the corresponding β -function. To this end we use the single-parameter scaling that implies $D_q(L) = D_q(t(L))$ and require that $D_q(t^*) = D_q^{(c)}$ given by Eq. (29), where t^* is the fixed point of RG equation Eq. (28).

Then expressing ϵ in terms of t^* from Eq. (28), plugging it in Eq. (29) and replacing t^* by $t = t(L)$ we obtain for $D(L) \equiv D_1(t(L))$:

$$1 - D = (2/d)(t + 8\zeta(3)t^4). \quad [30]$$

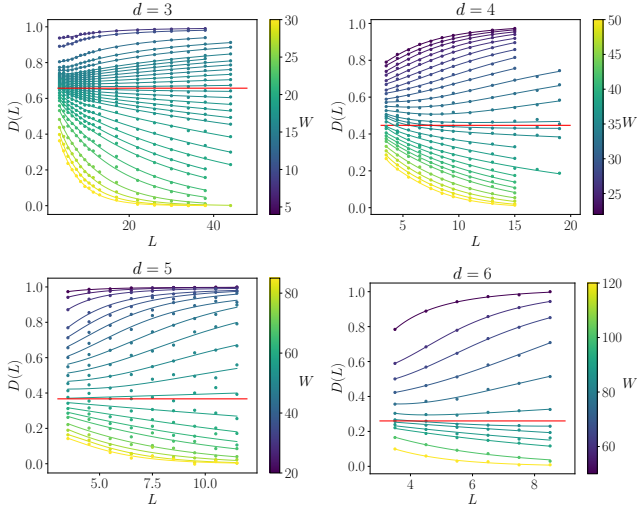


Fig. 6. System size dependence of the numerical fractal dimension at different dimensions $d = 3, 4, 5, 6$ and for different values of W . The solid lines are *interpolations* of the data, that we will use to produce the β -function. In particular, for $W < W_c$ we interpolate using a Padé function $D(L, d) = (L^{d-1} + aL^{d-2} + b)/(L^{d-1} + cL^{d-2} + k)$, while for $W > W_c$ we use $D(L) = \exp\{(-aL)\}/(bL + c)/(kL + m)$. These choices are dictated by physical arguments, namely the behavior of $\beta(D)$ at $D \sim 1$ and the exponential decay of D in the localized phase. The red lines in each plot represent the values of the critical fractal dimension obtained as the point at which the β -function vanishes, and that are reported in Table 1.

Differentiating Eq. (30) with respect to L^d , using the RG Eq. (28), expanding in $t \ll 1$ up to t^4 and using Eq. (30) we finally obtain:

$$\beta_D(D) = (1-D) \left(1 - \frac{2}{dD}\right) + 3d^2(d-2)\zeta(3)(1-D)^4 - \frac{d^2(24-d)}{4}\zeta(3)(1-D)^5 + O[(1-D)^6]. \quad [31]$$

At small $d-2 = \epsilon$ one can expand Eq. (31) up to quadratic order in $(1-D)$:

$$\beta_D(D) = (\epsilon/2)(1-D) - (1-D)^2 + O((1-D)^3). \quad [32]$$

Notice that the coefficient 1 of $(1-D)^2$ agrees with what is extracted from the numerical data (see Fig. 5 and Eq. (20)). This is an independent check of our numerical procedure. In this parabolic approximation the slopes of the β -function, α_c and α_1 , at $D = D_c$ (where $\beta_D(D_c) = 0$) and $D = 1$, obey the symmetry:

$$\alpha_c = -\alpha_1 = \frac{\epsilon}{2}. \quad [33]$$

However, this symmetry breaks down even in the ϵ^2 approximation when the subtle terms $\sim \zeta(3)$ are still neglected.

Self-consistent theory by Vollhardt and Woelfle and its violation. In the absence of the four-loop corrections proportional to $\zeta(3)$ the critical point D_c , the slope α_c of the β -function at $D = D_c$ and the critical exponent ν , Eq. (19), are found

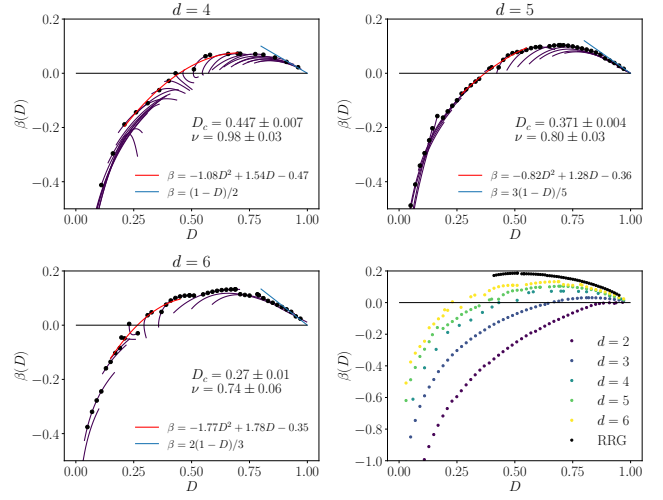


Fig. 7. Plots of the $\beta(D)$ for the Anderson localization model on higher-dimensional ($d = 4, 5, 6$) lattices. The colored lines are the numerical results, that are obtained from the participation entropy according to the definition. In particular, the fractal dimension is computed by applying the discrete derivative to S , and the resulting points are interpolated using a Padé fit for $W < W_c$ and an exponential fit for $W > W_c$ (see Fig. 6 for more details on the interpolations). The black points are a proxy for the envelope of the data, while the red curves are quadratic fits of the envelope of the numerical data around $\beta = 0$, from which we extract D_c and α_c as reported in the plots and Table 1. The blue line instead is the theoretical prediction for β near $D = 1$. The last plot is the set of envelopes for different dimensions and the RRG, displayed to highlight the flow for $d \rightarrow \infty$.

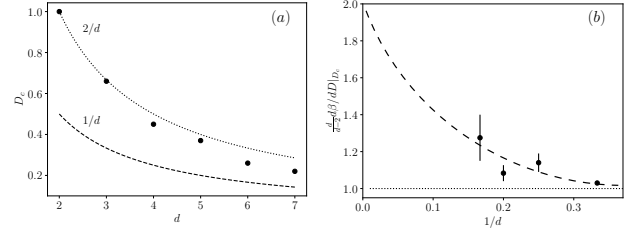


Fig. 8. (a) The critical fractal dimension D_c and (b) the ratio of slopes $d\beta_D/dD$ at $D = D_c$ and $D = 1$ as a function of d from exact diagonalization of the Anderson model on d -dimensional lattice. The last point $d = 7$ on the left panel is obtained with very restricted system sizes $L < 7$ and by a simplified method different from all other points. The dashed line in panel (b) qualitatively illustrates our conjecture, Eqs. (45),(46).

from Eq. (31) as:

$$D_c = \frac{2}{d}, \quad [34]$$

$$\alpha_c = \frac{d-2}{2}, \quad [35]$$

$$\nu = \frac{1}{d-2}. \quad [36]$$

This result coincides with the one of the so-called “self-consistent theory of localization” by Vollhardt and Woelfle (VW)(45). If Eqs. (34),(35),(36) were exact for some $d < d_{up}$, where d_{up} is an upper critical dimension, then inevitably $d_{up} = 4$, as for $d = 4$ the exponent ν takes its mean field value $\nu = 1/2$. Furthermore, at $d = 4$ within the VW theory, we obtain $D_c = 1/2$ which is the lower limit for D where two randomly chosen fractal wave functions intersect and thus can be correlated resulting in the Chalker’s scaling (46, 47).

As a matter of fact, the values of D_c at $d = 3$ and $d = 4$ match Eq. (34) pretty well (but D_c is smaller than $2/d$ for $d > 4$, see Table I). However, the value of $\nu \approx 1.57 - 1.59$ at $d = 3$, that is found numerically in Refs.(3, 27, 48, 49), differs substantially from the result of this theory $\nu = 1.0$, thus invalidating it. Therefore, there is no reason to trust the result of the VW theory, Eqs. (35),(36), according to which the slope α_c diverges in the limit $d \rightarrow \infty$.

Also, the values of α_c which we found and collected in Table I, are not described by Eq. (35). Surprisingly, for $d = 3, 4$ the values of α_c are very close to $-\alpha_1$ thus approximately exhibiting the symmetry Eq. (33) which should hold only at small $d - 2 = \epsilon$.

In fact, the contribution of the higher-order terms in the loop expansion in the nonlinear σ -model (the second term in Eq. (31)) makes the critical D_c smaller than $2/d$:

$$D_c = \frac{2}{d} - \frac{\zeta(3)}{8} \epsilon^4 + O(\epsilon^5), \quad [37]$$

The slope α_c and the ratio α_c/α_1 is also affected by these terms:

$$\alpha_c \equiv \left(\frac{d\beta_D}{dD} \right)_{D=D_c} = \frac{\epsilon}{2} + \frac{9}{8}\zeta(3)\epsilon^4 + O(\epsilon^5), \quad [38]$$

$$\alpha_1 \equiv \left(\frac{d\beta_D}{dD} \right)_{D=1} = -\frac{d-2}{d}, \quad [39]$$

$$\left| \frac{\alpha_c}{\alpha_1} \right| = 1 + \frac{\epsilon}{2} + \frac{9}{4}\zeta(3)\epsilon^3. \quad [40]$$

Notice that the product $\alpha_c D_c$ that determines the exponent ν reproduces the well-known result (28) obtained from the β -function for the variable t , Eq. (28):

$$\alpha_c D_c d = \nu^{-1} = \epsilon + \frac{9}{4}\zeta(3)\epsilon^4 + O(\epsilon^5). \quad [41]$$

This demonstrates the invariance of ν with respect to the change of variables $t(L) \rightarrow D(L)$ and provides proof of the correctness of our perturbative calculations.

Despite Eqs. (37)-(38) and Eqs. (40)-(41) are valid only at very small $\epsilon \lesssim 0.1$ and do not apply even for the case $d = 3$, the tendency they show is correct and observed in the numerical simulations [see Fig. 8(a,b)]. In particular, the fact that D_c decreases faster than $2/d$ with increasing d and that the ratio of the slopes obeys the following inequality:

$$\left| \frac{\alpha_c}{\alpha_1} \right| > 1, \quad [42]$$

and grows with increasing d , is convincingly confirmed.

Correlation between D_c and α_c and a ‘semi-classical theory’ for ν_d . As was already mentioned, the critical D_c for $d = 3, 4$ is very close to the result of the VW self-consistent theory $D_c = 2/d$. Next, we would like to note that the derivative of the β -function $\alpha_1 = -(d-2)/d$ at the fixed point $D = 1$ is an exact result of Eq. (31) which is independent of the higher-order terms in $(1-D)$. It is interesting to see what happens if $D_c = 2/d$ and the symmetry Eq. (33) is enforced beyond the lowest ϵ -expansion. The immediate consequence of $\alpha_c = |\alpha_1|$ is that the exponent $\nu = (dD_c\alpha_c)^{-1} = (dD_c|\alpha_1|)^{-1}$ would take the form:

$$\nu = \frac{d}{2(d-2)} = \frac{1}{2} + \frac{1}{d-2}. \quad [43]$$

Surprisingly, we obtained the formula empirically suggested by many authors (27, 50, 51), most notably in Ref. (50) where a sort of derivation is presented in the spirit of VW self-consistent theory. We think, however, that this ‘semiclassical theory’ is seriously flawed. In this derivation the momentum dependence of a Cooperon was changed from $\xi^2 q^2$ in the original VW paper to $D_0 \xi^2 q^d$, while the dependence of the correlation length ξ remained the same. This inevitably requires the dependence of $D_0 \propto \ell^{d-2}$ on the ultraviolet cutoff ℓ^{-1} which violates the single-parameter scaling. In contrast, our numerics demonstrates that the single-parameter scaling at $d = 3, 4, 5, 6$ is a very reasonable approximation.

Notwithstanding this comment, the values of ν obtained from Eq. (19) for $d = 3, 4, 5, 6$ using D_c and α_c found directly from the single-parameter β -function (see Fig. 7), are very close to the ones following from Eq. (43), obtained numerically in Ref. (51) and also experimentally in Ref. (52) for $d = 4$. At the same time, the values of D_c and α_c significantly differ from $2/d$ and $(d-2)/d$, respectively (see Fig. 8). This implies highly correlated deviations of these quantities from the above naive predictions.

We would like to stress that, in order to obtain a single-parameter curve, we employed a procedure that is completely different from the numerical approach of Refs.(3, 27, 48, 49, 53). In our approach, we extracted the single-parameter curve with no assumption on the number and values of the irrelevant exponents and then determined the relevant exponent ν from this single-parameter curve. This procedure is more complicated compared to that of Refs.(3, 27, 48, 49, 53) and it inevitably leads to less accurate numerical estimates of the exponents*. However, the clear advantage of this procedure is that it gives a detailed picture of the RG flow and emergence of single-parameter scaling and it is free from the choice of the number and values of the irrelevant exponents. In any case, the surprisingly high accuracy of a simple formula Eq. (43) for different dimensionalities $d = 3, 4, 5, 6$ raises again a question of its status and the approximation (which we think is still lacking) it can be obtained from.

A conjecture about the lower bound on D_c . In the absence of the upper critical dimension ($d_{up} = \infty$) it seems plausible that the exponent ν tends to $1/2$ in the limit $d \rightarrow \infty$, as was suggested by a number of authors (see e.g. Ref. (27)). Then the slope α_c in this limit can be found from Eq. (19) as:

$$\alpha_c = \frac{2}{D_c d}. \quad [44]$$

An immediate consequence of this is that α_c is finite in the $d \rightarrow \infty$ limit if D_c decreases with increasing the dimensionality d as $D_c \propto 1/d$ and this slope has an infinite limit if D_c decreases faster than $1/d$. Unfortunately, the numerical data up to $d = 7$ of Table 1 and Fig. 8 allows both asymptotic behaviors, with a crossover dimensionality that we estimate around $d^* \sim 10$. In this situation of the lack of theory at large d (when the non-linear sigma model is no longer justified) and the inability of numerical simulation on the lattices of dimensionality $d \gg d^*$ we would like to propose a conjecture on the lower bound for D_c for the Anderson

*Since the procedure involves finding the maximum of the numerical $\beta(D, L)$ in a given small interval $[D, D + \Delta D]$, for different L, W , we believe our procedure can lead to a *systematical overestimate* by a few percent the values of α_c, D_c and hence of ν .

model on d -dimensional lattices with short-range hopping. We argue that

$$D_c \geq \frac{1}{d}. \quad [45]$$

and if the upper critical dimension $d^{\text{up}} = \infty$ this inequality saturates only at $d = \infty$.

The reason for this conjecture is that by definition $D_c = d_c/d$, where d_c is the dimensionality of the support set of multifractal wave function embedded into a lattice of dimensionality d . Clearly, if $d_c < 1$ the support set cannot be connected and should look like a set of points with the typical distance between them much greater than the lattice constant. For a lattice model with short-range hopping, at high dimensions d the critical disorder $W_c \sim d \ln d$ is large. Therefore the typical transmission amplitude between such points should be exponentially small so that the points may belong to the same support set only if their on-site energies are in resonance with an exponential accuracy. This situation is extremely rare and this is exactly the point why we believe d_c must be greater than 1 if the wave function is extended and the model is short-ranged.

Certainly, this argument does not apply to systems with long-range hopping, e.g. for the Power-Law Banded random matrices (54) or the Rosenzweig-Porter models (39, 40, 55). In those cases, $d = 1$ and it is known that $d_c < 1$ can be arbitrarily small.

If the conjecture Eq. (45) is true then Eq. (44) immediately gives:

$$\lim_{d \rightarrow \infty} \alpha_c = 2, \quad [46]$$

that is, it is (a) finite and (b) twice larger than $\lim_{d \rightarrow \infty} \alpha_1 = 1$. This seemingly innocuous conclusion has an important implication for the critical scaling of the Anderson model on Random Regular Graphs (RRG). If, in fact, $\beta(D)_{\text{RRG}} = \lim_{d \rightarrow \infty} \beta(D)_d$, then this allows us to choose scenario I formulated in Ref. (1) as the only possible, and therefore the RRG has two diverging lengths as $W \rightarrow W_c$: one with exponent $\nu = 1/2$ and one with exponent $\nu = 1$, which dominates (although sizes larger than the available ones are needed to observe $\nu = 1$ in the numerical data). The existence of two critical exponents was also discussed, in a different context, in Ref. (56).

The high-gradient operators in the non-linear sigma-model and the irrelevant exponent y

As is seen from Fig. 7, the single-parameter scaling is an approximation that corresponds to the *envelope* of RG trajectories shown by a solid red line around $\beta = 0$. A given RG trajectory (shown by a solid black line) approaches this envelope at a sufficiently large system size L . To describe the initial part of RG trajectories one needs to invoke an *irrelevant exponent* y introduced in Ref. (48). Apparently, this exponent is *beyond* the single-parameter scaling as described by the formalism of the non-linear sigma model (43, 44, 57).

In order to understand the origin of the operators corresponding to the exponent y one has to *extend* the conventional sigma-model (57, 58). The corresponding extension was done in Ref. (32, 33, 59) by adding to the sigma-model, in addition to the conventional ‘diffusion’ term $t^{-1} \text{Str}[(\nabla Q)^2]$, also the higher-order ($n > 1$) terms of the gradient expansion:

$$Z_n \ell^{2(n-1)} \text{Str}[(\nabla Q)^{2n}], \quad [47]$$

where Q is the Efetov’s super-matrix (58), ℓ is the electron mean free path and Str denotes the super-trace. Such terms can be rigorously derived (32, 33, 59) starting from the model of free electrons in impure metals.

The additional terms have an irrelevant exponent $y_n^{(0)} = -2(n-1)$ in the zero-order approximation of non-interacting diffusion modes (the conventional term proportional to $(\nabla Q)^2$ has an exponent 0 in this approximation). The interaction of diffusion modes leads to a renormalization of the coupling constant t described by one-parameter scaling, Eq. (28). However, it also gives rise (32, 33, 59) to renormalization of Z_n in Eq. (47):

$$\frac{d \ln Z_n}{du} = n(n-1) + \text{higher order in } t \sim \epsilon, \quad [48]$$

where

$$u = \ln \left(\frac{\sigma_0}{\sigma(L)} \right) = \frac{(L/\ell)^\epsilon}{1 + (L/\xi)^\epsilon}. \quad [49]$$

Here $\epsilon = d - 2$, ξ is the critical length, σ_0 is the Drude conductivity, and $\sigma(L)$ is that with effects of localization included.

At small ϵ one may neglect the higher-order terms in $t \sim \epsilon$ in Eq. (48), so that:

$$Z_n = Z_n^{(0)} \left[\frac{(L/\ell)^\epsilon}{1 + (L/\xi)^\epsilon} \right]^{n(n-1)}. \quad [50]$$

At criticality, $L \ll \xi$, the L -dependent term in the denominator of Eq. (50) can be neglected and we obtain $Z_n \propto L^{\epsilon n(n-1)}$. This gives a *positive* correction to y_n (see also Fig. 10):

$$y_n = -2(n-1) + \epsilon n(n-1) + o(\epsilon). \quad [51]$$

At $\epsilon \ll 1$ the largest irrelevant exponent corresponds to $n = 2$, so that we obtain:

$$y = y_2 = -2 + 2\epsilon + o(\epsilon). \quad [52]$$

Equation (52) shows that the irrelevant exponent $y > -2$ (which is always the case in numerics (49)) and grows with increasing the dimensionality $\epsilon = d - 2$. As usual in ϵ -expansion in the localization problem, this equation is not applicable already for $d = 3$. However, it shows a tendency towards making the irrelevant exponent less irrelevant with increasing d . This results in the corrections to single-parameter scaling (and hence the length of the RG trajectories before merging with the single-parameter red curve, see Fig. 7) more significant, as d increases.

What happens at large d ? One of the possibilities is that the irrelevant exponent becomes relevant (positive) at some finite $d = d^{\text{up}}$ and the single-parameter scaling will no longer hold for $d > d^{\text{up}}$, even as an approximation. We, however, think that $d^{\text{up}} = \infty$ and the breakdown of the single-parameter scaling happens only for localization problems on expander graphs like RRG (1).

We would like to emphasize that the scenario of breakdown of single parameter scaling at $d > d^{\text{up}}$ described above is different from the one suggested recently by Zirnbauer (30, 60). The true theory of the NEE phase with singular-continuous spectrum should, perhaps, be a combination of both, in which the higher-gradient terms should play an important role.

d	W_c	D_c	$\alpha_c d$	$\nu = \frac{1}{\alpha_c d D_c}$	ν_{num}	ν , Eq. (43)
3	16.4 ± 0.2	0.657 ± 0.001	1.029 ± 0.01	1.48 ± 0.02	1.57 ± 0.004 (53), 1.52 ± 0.06 (51)	$3/2$
4	34.3 ± 0.2	0.447 ± 0.007	2.28 ± 0.10	0.98 ± 0.03	1.156 ± 0.014 (27), 1.03 ± 0.07 (51)	1
5	56.5 ± 0.5	0.367 ± 0.004	3.25 ± 0.13	0.84 ± 0.03	0.969 ± 0.015 (27), 0.84 ± 0.06 (51)	$5/6 \approx 0.83$
6	83.5 ± 0.5	0.26 ± 0.01	5.1 ± 0.5	0.74 ± 0.06	0.78 ± 0.06 (51)	$3/4$
7	110 ± 2	0.22 ± 0.04	/	/	/	/

Table 1. Numerical values for critical properties in $d = 3, 4, 5, 6$, compared with previous results in the literature. The values of W_c we find, corresponding to the red lines in Fig. 6, are compatible with the results in the literature (5, 53). The values of D_c and critical exponents are found by analyzing the numerical data around $\beta = 0$. The errors displayed are the ones coming from a quadratic fit of the envelope of the β -function near the critical point (red curve in the plots). We expect the actual errors to be larger than the ones reported.

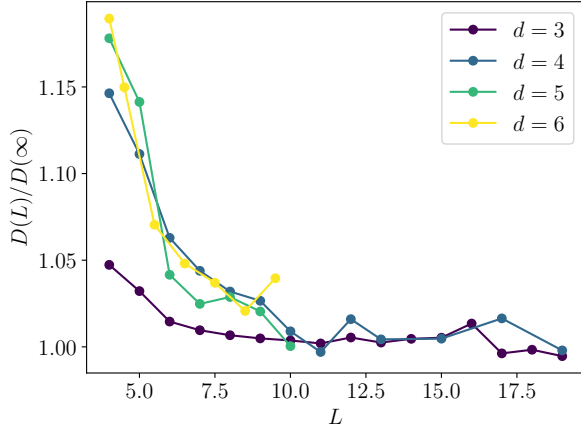


Fig. 9. System size dependence of $D(L)/D(L \rightarrow \infty)$ at $W = W_c$ for different spatial dimensions. When d increases, also $D(L = O(1))/D(L \rightarrow \infty)$ grows, that implies a longer length of the “hair” in the β -function. However, the saturation value is achieved approximately at the same linear size $L = O(10)$, as we discuss in the main text.

Approaching the critical point

One can see from our numerics (Figs. 1, 7) that $D(L)$ has a minimum D_A which corresponds to $\beta(D_A) = 0$ (see the sketch on the upper panel of Fig. 2). It is natural to ask how the minimum of $D(L)$ is approached in different dimensions. As it happens on the Random Regular Graph (1), the β -function crosses the line $\beta = 0$ with infinite derivative, therefore the simplest approximation for the $\beta(D)$ is

$$\beta(D) \simeq -\sqrt{D - D_A}, \quad [53]$$

where $\beta(D_A) = 0$. By straightforwardly integrating the differential equation (9) it is easy to get for the volume $V_A = L_A^d$ that corresponds to the minimum D_A :

$$V_A = V_0 \exp \left\{ \frac{2 \arccos \sqrt{D_A/D_0}}{\sqrt{D_A}} \right\} \quad [54]$$

In the above equation, V_0 and D_0 represent the initial condition and we can take $V_0 < V_A$ to be independent of d , while in general $D_0 = D_0(d) > D_A$. We now move to the regime $W \lesssim W_c$ and let us assume d is large enough so that $D_A \gtrsim D_c \sim 1/d \ll 1$. In this regime, we can expand Eq. (54)

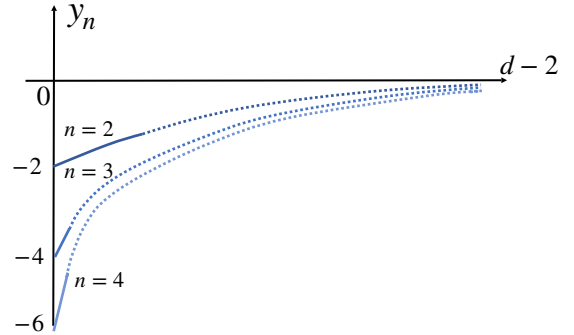


Fig. 10. Dependence of the irrelevant exponents y_n on the spatial dimension of the system. The solid lines represent Eq. (51), while the dashed lines give a sketch of our conjecture as d increases. We conjecture that in the limit of large d all dashed lines merge and approach zero.

in D_A/D_0 and we get

$$V_A = V_0 \exp \left\{ \left(\frac{\pi}{\sqrt{D_A}} - \frac{2}{\sqrt{D_0}} \right) \right\} = \tilde{V}_0 \exp \left\{ \left(\frac{\pi}{\sqrt{D_A}} \right) \right\} \quad [55]$$

$$\simeq \tilde{V}_0 \exp \{ (c\sqrt{d}) \}, \quad [56]$$

where $c = O(1)$ is a constant. Note that the system volume where the minimum is reached is finite in the limit $D_A \rightarrow D_c$. Thus in any finite dimension d the length $L_A = V_A^{1/d}$ that corresponds to the volume V_A is not critical, in (at least qualitative) agreement with the data in Fig. 9. Moreover, it is equal to the volume $\tilde{V}_0 = O(1)$ in the limit $d \rightarrow \infty$. This is in contrast to the case of RRG where the corresponding length is critical $L_A \sim (W_c - W)^{-1/2}$. This is the consequence of the difference in the dependence of the volume on the length on a d -dimensional lattice and on a tree/RRG with finite branching number K_0 . Indeed, if the relation between the volume V_A and the length L_A were like on a tree/RRG then we would obtain from Eq. (56) a divergent length $L_A = \ln(V_A)/\ln K_0 \sim \sqrt{d}$ in the double limit $D_A \rightarrow D_c$ and $d \rightarrow \infty$.

In any case, the result that the length $L_A \sim O(1)$ in any finite dimensions implies that the critical length is associated with the single-parameter part of the trajectory and is given by Eq. (18) with $D_0 \approx D_A$. In contrast, on the RRG there are two critical lengths, provided that the slope α_c is finite: one of them is $L_A = (W_c - W)^{-1/2}$ and the other, the dominant one, is determined by the single-parameter part of the β -function. In this case the exponent $\nu = 1$ independently of the (finite) slope α_c .

This analysis tells us that the localization transition on the expander graphs like RRG is not simply that in the

limit $d \rightarrow \infty$ on a d -dimensional lattice. A qualitative jump happens in the critical behavior because the single-parameter character of the transition in d -dimensions is replaced by a two-parameter one on expander graphs (1).

Increasing space dimensionality and the Random Regular Graph

In the previous sections, we have described in detail the behavior of the β -function for the Anderson model in finite dimensions, comparing our theoretical arguments with the numerical results from exact diagonalization.

The goal of this section is to summarize our knowledge and conjectures concerning the scaling behavior on a d -dimensional lattice in the limit $d \rightarrow \infty$.

- Let us first focus on the region $D \rightarrow 1$. As we already discussed, in d dimensions the β -function in this limit has slope $\alpha_1 = (d-2)/d$ (see Eq. (39)). For $d \rightarrow \infty$ this readily gives $\alpha_1 = 1$, which is the prediction of RMT and is found in the Anderson model on RRG.
- We have seen numerically that the critical value of the fractal dimension $D_c \leq 2/d$, and we have argued that there are reasons to believe that $D_c \geq 1/d$ for any d . Independently from the lower bound, $D_c \rightarrow 0$ as $d \rightarrow \infty$, in agreement with the results on expander graphs (1, 10).
- As shown in Fig. 1 and Fig. 9 and schematically sketched in Fig. 2, the contribution of the irrelevant operators at the critical point becomes increasingly important as d grows (as evident from the length of the ‘‘hairs’’ in $\beta(D)$). This implies that the irrelevant exponents become less irrelevant with increasing d until, eventually, a two-parameter scaling emerges for expander graphs like RRG.
- The critical behavior on a d -dimensional lattice, and even in the limit $d \rightarrow \infty$, is qualitatively different from that on an expanded graph like RRG. On a lattice of any dimension, it takes a finite length (sample size) to reach the minimum of $D(L)$ when $\beta(D) = 0$, even as we approach the critical disorder. In contrast, this length diverges at $W \rightarrow W_c$ as $(W_c - W)^{-1/2}$ on RRG.
- The sample size L_c when the true metallic behavior $D \approx 1$ is reached for $W < W_c$ is critically divergent $L_c = (W_c - W)^{-\nu}$ in both cases. It is determined by the single-parameter part of the β -function. However, for the case of a d -dimensional lattice the exponent $\nu = 1/(dD_c\alpha_c)$ depends both on the critical value of D_c and on the slope α_c of the β -function and in the limit $d \rightarrow \infty$ reaches the mean field value $\nu = 1/2$. In contrast, on RRG (where $D_c = 0$), $\nu = 1$ independently of the slope α_c , provided that the slope is finite. This crucial difference is due to the qualitative change in the scaling, which is two-parameter with $D_c = 0$ for RRG (1) and single-parameter with $D_c > 0$ and corrections due to irrelevant operators for d -dimensional lattice.

Role of loops and correlations in infinite dimensions

One of the outcomes of our work is that the single-parameter $\beta(D) > 0$ (a ‘single-parameter arc’) for RRG (1) is a smooth

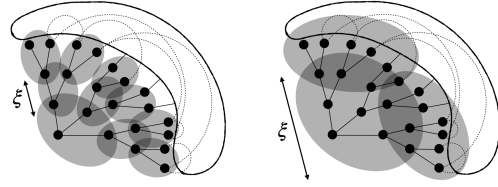


Fig. 11. Pictorial representation of an RRG and the size of correlations at different disorder strengths. For small W (left), the correlation length is small, and under real space RG, the limit $\xi/L \simeq 0$ is soon achieved, leading to RMT. For larger W , ξ is larger, possibly leading to the failure of resonance hybridization, depending on the graph structure.

deformation of the corresponding arc for $D > D_c$ on d -dimensional lattice as d increases and tends to infinity. On the other hand, it is known that in the absence of loops (i.e. on a tree) the Anderson model (with one orbital per site) displays multifractality in the entire delocalized phase (7, 61), where $0 < D < 1$ in the thermodynamic limit. The corresponding β -function must, therefore, terminate somewhere on the line $\beta(D) = 0$ depending on the initial conditions (e.g. the strength of disorder W). This means that the single parameter arc in the case of a loopless tree is absent. Instead, there is a line of fixed points $[0, 1]$ where the two-parameter RG trajectories terminate. This is a strong indication that the single-parameter arc (along which the system evolves to the ergodic fixed point) emerges due to the loops on a corresponding graph.

Indeed, let us consider an expander graph of diameter L and connectivity K , so that its volume is $N = K^L$. In the ergodic phase, let us denote the correlation length with ξ , defined as the characteristic length scale for the decay of the two-point function. Upon averaging, ξ is a function of the disorder strength: at small W , ξ is small, since the system is chaotic; on the other hand, when approaching the critical point at $W = W_c$, ξ diverges (see Fig. 11), as it is expected at a phase transition. The correlation length ξ can also be interpreted as the typical distance between resonances. In the localized phase the relevant length scale becomes the localization length. When $\xi = O(1)$ resonances are very close, and under real space RG (or increasing system size) the regime $\xi/L \sim 0$ is soon achieved. The system behaves as a fully connected quantum dot and exhibits random matrix properties. By increasing W , the distance between resonances grows, and they can eventually fail to hybridize. Their fate, though, depends on the properties of the graph. On a tree, the sites on the ‘leaves’ at remote branches are at a large distance from each other, as they can be connected only through the root (see right panel of Fig. 12). However, RRGs are characterized by the presence of large-scale loops connecting such sites and providing the shortcuts thereby (see left panel of Fig. 12). This means that the loops help in boosting the hybridization of resonances, reversing the RG flow and making it go to RMT along the single-parameter arc (see Fig. 2).

Conclusions

In this work, we presented a renormalization group-based framework for addressing the Anderson localization transition in finite dimension. We discussed how to use the ‘modern’ observables to construct the full β -function of the model in

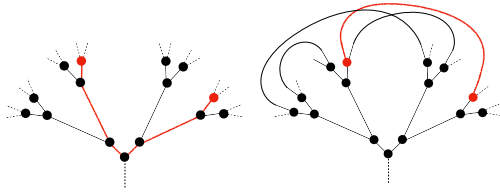


Fig. 12. Resonances (pictorially represented as red dots) that are far apart on a tree (left) can become close on the RRG because of loops (right). This phenomenon facilitates the flow towards ergodicity, removing the fractal phase on the RRG.

any spatial dimension d . For practical purposes, we chose the finite size fractal dimension $D(N)$ as such an observable, albeit other (eigenfunction or spectral) observables can do the same job as long as one-parameter scaling holds. We showed that some basic properties can be derived analytically by simple arguments and, when this was not possible, we presented numerical results from which we derived critical properties, in agreement with previous results in the literature. More importantly, we showed how our technique connects the perturbative results in $d = 2 + \epsilon$ dimensions up to $d \rightarrow \infty$, recovering the known results on RRGs, where this method has been applied recently (1).

We believe that the method discussed here, and already applied to expander graphs, is a new useful tool to understand the scaling properties of *ergodicity breaking* in disordered quantum systems, and especially to study the existence and properties of such purported transitions. This is of particular importance for interacting systems where the existence and the properties of non-ergodic phases are under long-standing debate.

ACKNOWLEDGMENTS. V.E.K. is grateful to Misha Feigelman for fruitful discussions and support from Google Quantum Research Award “Ergodicity breaking in Quantum Many-Body Systems”. V.E.K. is grateful to KITP, University of Santa Barbara for hospitality. This research was supported in part by the National Science Foundation under Grant No. NSF PHY-1748958. A.S. acknowledges financial support from the National Recovery and Resilience Plan (NRRP), Mission 4 Component 2 Investment 1.3 funded by the European Union NextGenerationEU. National Quantum Science and Technology Institute (NQSTI), PE00000023, Concession Decree No. 1564 of 11.10.2022 adopted by the Italian Ministry of Research, CUP J97G22000390007. P.S. acknowledges support from ERC AdG NOQIA; MCIN/AEI (PGC2018-0910.13039/501100011033, CEX2019-000910-S/10.13039/501100011033, Plan National FIDEUA PID2019-106901GB-I00, Plan National STAMEENA PID2022-139099NB-I00 project funded by MCIN/AEI/10.13039/501100011033 and by the “European Union NextGenerationEU/PRTR” (PRTR-C17.11), FPI); QUANTERA MAQS PCI2019-111828-2); QUANTERA DYNAMITE PCI2022-132919 (QuantERA II Programme co-funded by European Union’s Horizon 2020 program under Grant Agreement No 101017733), Ministry of Economic Affairs and Digital Transformation of the Spanish Government through the QUANTUM ENIA project call - Quantum Spain project, and by the European Union through the Recovery, Transformation, and Resilience Plan - NextGenerationEU within the framework of the Digital Spain 2026 Agenda; Fundació Cellex; Fundació Mir-Puig; Generalitat de Catalunya (European Social Fund FEDER and CERCA program, AGAUR Grant No. 2021 SGR 01452, QuantumCAT U16-011424, co-funded by ERDF Operational Program of Catalonia 2014-2020); Barcelona Supercomputing Center MareNostrum (FI-2023-2-0024); EU Quantum Flagship (PASQuanS2.1, 101113690); EU Horizon 2020 FET-OPEN OPTologic (Grant No 899794); EU Horizon Europe Program (Grant Agreement 101080086 - NeQST), ICFO

Internal “QuantumGaudi” project; European Union’s Horizon 2020 program under the Marie Skłodowska-Curie grant agreement No 847648; “La Caixa” Junior Leaders fellowships, “La Caixa” Foundation (ID 100010434): CF/BQ/PR23/11980043. Views and opinions expressed are, however, those of the author(s) only and do not necessarily reflect those of the European Union, European Commission, European Climate, Infrastructure and Environment Executive Agency (CINEA), or any other granting authority. Neither the European Union nor any granting authority can be held responsible for them.

1. C Vanoni, BL Altshuler, VE Kravtsov, A Scardicchio, Renormalization group analysis of the anderson model on random regular graphs. *arXiv* (2023).
2. PW Anderson, Absence of diffusion in certain random lattices. *Phys. Rev.* **109**, 1492–1505 (1958).
3. T Ohtsuki, K Slevin, T Kawarabayashi, Review of recent progress on numerical studies of the anderson transition. *Annalen der Physik* **511**, 655–664 (1999).
4. F Evers, AD Mirlin, Anderson transitions. *Rev. Mod. Phys.* **80**, 1355 (2008).
5. E Tarquini, G Biroli, M Tarzia, Critical properties of the anderson localization transition and the high-dimensional limit. *Phys. Rev. B* **95**, 094204 (2017).
6. M Baroni, GG Lorenzana, T Rizzo, M Tarzia, Corrections to the bethe lattice solution of anderson localization. *arXiv preprint arXiv:2304.10365* (2023).
7. KS Tikhonov, AD Mirlin, Fractality of wave functions on a cayley tree: Difference between tree and locally treelike graph without boundary. *Phys. Rev. B* **94**, 184203 (2016).
8. KS Tikhonov, AD Mirlin, MA Skvortsov, Anderson localization and ergodicity on random regular graphs. *Phys. Rev. B* **94**, 220203 (2016).
9. S Bera, G De Tomasi, IM Khaymovich, A Scardicchio, Return probability for the anderson model on the random regular graph. *Phys. Rev. B* **98**, 134205 (2018).
10. P Sierant, M Lewenstein, A Scardicchio, Universality in anderson localization on random graphs with varying connectivity. *SciPost Phys.* **15**, 045 (2023).
11. I Garcia-Mata, et al., Critical properties of the anderson transition on random graphs: Two-parameter scaling theory, kosterlitz-thouless type flow, and many-body localization. *Phys. Rev. B* **106**, 214202 (2022).
12. D Basko, I Aleiner, B Altshuler, Metal–insulator transition in a weakly interacting many-electron system with localized single-particle states. *Ann. Phys.* **321**, 1126–1205 (2006).
13. R Nandkishore, DA Huse, Many-body localization and thermalization in quantum statistical mechanics. *Annu. Rev. Condens. Matter Phys.* **6**, 15–38 (2015).
14. DA Abanin, E Altman, I Bloch, M Serbyn, Colloquium: Many-body localization, thermalization, and entanglement. *Rev. Mod. Phys.* **91**, 021001 (2019).
15. V Ros, M Müller, A Scardicchio, Integrals of motion in the many-body localized phase. *Nucl. Phys. B* **891**, 420–465 (2015).
16. JZ Imbrie, V Ros, A Scardicchio, Local integrals of motion in many-body localized systems. *Ann. Phys.* **529**, 1600278 (2017).
17. M Žnidarič, A Scardicchio, VK Varma, Diffusive and subdiffusive spin transport in the ergodic phase of a many-body localizable system. *Phys. Rev. Lett.* **117**, 040601 (2016).
18. BL Altshuler, Y Gefen, A Kamenev, LS Levitov, Quasiparticle lifetime in a finite system: A nonperturbative approach. *Phys. Rev. Lett.* **78**, 2803–2806 (1997).
19. A De Luca, B Altshuler, V Kravtsov, A Scardicchio, Anderson localization on the bethe lattice: Nonergodicity of extended states. *Phys. review letters* **113**, 046806 (2014).
20. K Tikhonov, A Mirlin, From anderson localization on random regular graphs to many-body localization. *Ann. Phys.* **435**, 168525 (2021).
21. J Šuntajs, J Bonča, T Prosen, L Vidmar, Quantum chaos challenges many-body localization. *Phys. Rev. E* **102**, 062144 (2020).
22. RK Panda, A Scardicchio, M Schulz, SR Taylor, M Žnidarič, Can we study the many-body localisation transition? *EPL (Europhysics Lett.)* **128**, 67003 (2020).
23. D Abanin, et al., Distinguishing localization from chaos: Challenges in finite-size systems. *Annals Phys.* **427**, 168415 (2021).
24. P Sierant, D Delande, J Zakrzewski, Thouless time analysis of anderson and many-body localization transitions. *Phys. Rev. Lett.* **124**, 186601 (2020).
25. P Sierant, J Zakrzewski, Challenges to observation of many-body localization. *Phys. Rev. B* **105**, 224203 (2022).
26. R Abou-Chacra, D Thouless, P Anderson, A selfconsistent theory of localization. *J. Phys. C: Solid State Phys.* **6**, 1734 (1973).
27. Y Ueoka, K Slevin, Dimensional dependence of critical exponent of the anderson transition in the orthogonal universality class. *J. Phys. Soc. Jpn.* **83**, 084711 (2014).
28. S Hikami, Localization, nonlinear σ model and string theory. *Prog. Theor. Phys. Suppl.* **107**, 213–227 (1992).
29. Y Ueoka, K Slevin, Borel–padé re-summation of the β -functions describing anderson localisation in the wigner–dyson symmetry classes. *J. Phys. Soc. Jpn.* **86**, 094707 (2017).
30. J Arenz, MR Zirnbauer, Wegner model on a tree graph: U (1) symmetry breaking and a non-standard phase of disordered electronic matter. *arXiv* (2023).
31. E Abrahams, PW Anderson, DC Licciardello, TV Ramakrishnan, Scaling theory of localization: Absence of quantum diffusion in two dimensions. *Phys. Rev. Lett.* **42**, 673–676 (1979).
32. BL Altshuler, VE Kravtsov, IV Lerner, Statistical properties of mesoscopic fluctuations and similarity theory. *JETP Lett.* **43**, 441 (1986).
33. BL Altshuler, VE Kravtsov, IV Lerner, Statistics of mesoscopic fluctuations and instability of one-parameter scaling. *Zh. Eksp. Teor. Fiz.* **91**, 2276 (1986).
34. PA Lee, DS Fisher, Anderson localization in two dimensions. *Phys. Rev. Lett.* **47**, 882–885 (1981).
35. JT Chalker, VE Kravtsov, IV Lerner, Spectral rigidity and eigenfunction correlations at the anderson transition. *J. Exp. Theor. Phys. Lett.* **64**, 386–392 (1996).

36. E Bogomolny, O Giraud, C Schmit, Integrable random matrix ensembles. *Nonlinearity* **24**, 3179–3213 (2011).
37. E Bogomolny, O Giraud, Eigenfunction entropy and spectral compressibility for critical random matrix ensembles. *Phys. Rev. Lett.* **106**, 044101 (2011).
38. V Oganessian, DA Huse, Localization of interacting fermions at high temperature. *Phys. review b* **75**, 155111 (2007).
39. VE Kravtsov, IM Khaymovich, E Cuevas, M Amini, A random matrix model with localization and ergodic transitions. *New J. Phys.* **17**, 122002 (2015).
40. IM Khaymovich, VE Kravtsov, BL Altshuler, LB Ioffe, Fragile ergodic phases in logarithmically-normal Rosenzweig-Porter model. *Phys. Rev. Res.* **2**, 043346 (2020).
41. PA Lee, T Ramakrishnan, Disordered electronic systems. *Rev. modern physics* **57**, 287 (1985).
42. J Šuntajs, T Prosen, L Vidmar, Localization challenges quantum chaos in the finite two-dimensional anderson model. *Phys. Rev. B* **107**, 064205 (2023).
43. F Wegner, Anomalous dimensions for the nonlinear sigma-model in 2+epsilon dimensions. *Nucl. Phys. B* **280**, 210 (1987).
44. F Wegner, Four-loop-order beta-function of nonlinear sigma-models in symmetric spaces. *Nucl. Phys. B* **316**, 663 (1989).
45. P Wölfle, D Vollhardt, Self-consistent theory of anderson localization: General formalism and applications. *Int. J. Mod. Phys. B* **24**, 1526–1554 (2010).
46. JT Chalker, GJ Daniel, Scaling, diffusion, and the integer quantized hall effect. *Phys. Rev. Lett.* **61**, 593 (1988).
47. JT Chalker, Scaling and eigenfunction correlations near a mobility edge. *Phys. A: Stat. Mech. its Appl.* **167**, 253 (1990).
48. K Slevin, T Ohtsuki, Corrections to scaling at the anderson transition. *Phys. Rev. Lett.* **82**, 382–385 (1999).
49. A Rodrigues, L Vasquez, K Slevin, RA Roemer, Multifractal finite-size scaling and universality at the anderson transition. *Phys. Rev. B* **84**, 134209 (2011).
50. AM Garcia-Garcia, Semiclassical theory of the anderson transition. *Phys. Rev. Lett.* **100**, 076404 (2008).
51. AM Garcia-Garcia, E Cuevas, Dimensional dependence of the metal-insulator transition. *Phys. Rev. B* **75**, 074203 (2007).
52. F Madani, et al., Exploring quantum criticality in a 4d quantum disordered system. *arXiv preprint 2402.06573* (2024).
53. K Slevin, T Ohtsuki, Critical exponent for the anderson transition in the three-dimensional orthogonal universality class. *New J. Phys.* **16**, 015012 (2014).
54. AD Mirlin, YV Fyodorov, FM Dittes, J Quezada, TH Seligman, Transition from localized to extended eigenstates in the ensemble of power-law random banded matrices. *Phys. Rev. E* **54**, 3221 (1996).
55. A Kuttlin, C Vanoni, Investigating finite-size effects in random matrices by counting resonances. *arXiv:2402.10271* (2024).
56. I Garcia-Mata, et al., Two critical localization lengths in the anderson transition on random graphs. *Phys. Rev. Res.* **2**, 012020 (2020).
57. F Wegner, The mobility edge problem: continuous symmetry and a conjecture. *Zeitschrift für Physik B Condens. Matter* **35**, 207–210 (1979).
58. K.B.Efetov, Supersymmetry and theory of disordered metals. *Adv. Phys.* **32**, 53 (1983).
59. BL Altshuler, VE Kravtsov, IV Lerner, *Mesoscopic phenomena in solids*. (Elsevier), p. 449 (1991).
60. MR Zirnbauer, Wegner model in high dimension: U(1) symmetry breaking and a non-standard phase of disordered electronic matter, i. one-replica theory. *arXiv* (2023).
61. V Kravtsov, B Altshuler, L Ioffe, Non-ergodic delocalized phase in anderson model on bethe lattice and regular graph. *Ann. Phys.* **389**, 148–191 (2018).